European Archives of Oto-Rhino-Laryngology (2019) 276:2705–2714
https://doi.org/10.1007/s00405-019-05511-8

OTOLOGY

Clinicoradiologic characteristics of endolymphatic sac tumors

Hongbo Le[1] · Huihong Zhang[2] · Weijing Tao[3] · Lan Lin[4,5] · Jie Li[6] · Lin Ma[4] · Guobin Hong[1] · Xin Lou[4]

Received: 12 March 2019 / Accepted: 8 June 2019 / Published online: 13 June 2019

Abstract

Purpose Endolymphatic sac tumor (ELST) is a rare, slow-growing, and low-grade malignant tumor arising from the endolymphatic sac in the posterior petrous bone. The purpose of this study is to describe the clinical and radiologic features, and investigate the clinicoradiologic correlation of ELST.

Methods We retrospectively reviewed the clinical, computed tomography (CT), magnetic resonance imaging (MRI), and pathologic findings of 14 patients with 15 ELSTs.

Results Patients comprised of eight women and six men with a mean age of 42.3 years at the time of diagnosis and 35.2 years at the time of initial symptoms. The mean interval between initial symptoms and diagnosis was 84.7 months. The most frequent cochleovestibular symptom was hearing loss in 14 patients (100%); other cochleovestibular symptoms were tinnitus in eight patients (57.1%), vertigo in three patients (21.4%), and aural fullness in three patients (21.4%). Ten patients (71.4%) presented with facial paralyses and five patients (14.3%) presented lower cranial nerve deficits. CT findings revealed spiculated, stippled, or reticular high density within the tumors. The lesions involved mastoid cells, vertical facial nerve canal, semicircular canal, cochlea, tympanum, jugular foramen, internal auditory canal, or petrous apex. On the available MRI, all the eight lesions showed patchy and/or speckled hyperintensity on unenhanced T1WI. Five lesions showed flow voids on T2WI and T1WI. Three lesions had blood fluid levels within cysts.

Conclusion CT and MRI findings of ELSTs are associated with clinical features. Imaging tests should be performed to identify ELSTs early and ensure greater potential for hearing preservation in patients with cochleovestibular symptoms.

Keywords Endolymphatic sac tumor · Computed tomography · Magnetic resonance imaging · Petrous bone

✉ Guobin Hong
honggb@mail.sysu.edu.cn

✉ Xin Lou
louxin@301hospital.com.cn

1 Department of Radiology, The Fifth Affiliated Hospital of Sun Yat-Sen University, 52# Meihua Dong Road, Zhuhai 519000, China

2 Food Safety and Health Research Center, School of Public Health, Southern Medical University, Guangzhou 510515, China

3 Department of Radiology, The Affiliated Huai'an No.1 People's Hospital of Nanjing Medical University, Huai'an 223300, China

4 Department of Radiology, Chinese People's Liberation Army (PLA) General Hospital, 28# Fuxing Road, Beijing 100853, China

5 Department of Radiology, Dongsheng People's Hospital, Erdos 017000, Inner Mongolia, China

6 Department of Pathology, Chinese People's Liberation Army (PLA) General Hospital, Beijing 100853, China

Introduction

Endolymphatic sac tumor (ELST) is a rare, low-grade malignant epithelial tumor arising from the endolymphatic sac in the temporal bone [1]. It is a slow-growing, locally aggressive neoplasm that destroys the temporal bone and exhibits a papillary glandular appearance [2, 3]. In 1984, Hassard and his colleagues [4] described the first case of ELST. In 1988, Gaffey et al. [5] recognized a locally destructive tumor of the temporal bone in the region of the endolymphatic sac, and classified such tumor into the more aggressive papillary adenoma distinct from middle ear adenoma. In 1989, Heffner [6] reported a series of 20 patients with papillary epithelial tumors of the temporal bone with an epicenter at the posteromedial petrous bone where the endolymphatic sac resides. In 1993, Li et al. [7] proposed a reclassification of these aggressive adenomatous papillary neoplasms as endolymphatic sac tumors. It was Heffner who provided evidence that these aggressive tumors arise from the endolymphatic

sac, so ELST was also called Heffner's tumor. These tumors can occur sporadically or be a part of von Hippel–Lindau (VHL) syndrome, an autosomal dominant disease predisposing to a variety of lesions, such as hemangioblastomas of the retina and central nervous system (CNS), pheochromocytomas, clear cell renal cell carcinomas, pancreatic neuroendocrine tumors, and pancreatic cystadenomas [8–10].

In this article, we reported 14 patients with ELSTs regarding the clinical and radiographic features with the pathologic findings and a review of the literature.

Materials and methods

This was a retrospective study on 14 patients with 15 ELSTs (bilateral tumors in 1 case) between August 2008 and June 2018. The clinical, radiographic, surgical, and pathologic findings were retrieved and reviewed. This study was approved by the Ethics Committee of the Fifth Affiliated Hospital of Sun Yat-sen University.

Clinical findings included patient's age, the time between the initial onset of symptoms and diagnosis, the clinical symptoms at presentation, and a family of VHL disease.

All the patients underwent high-resolution computed tomography (HRCT) scanning and magnetic resonance imaging (MRI) scanning for the radiological assessment before the surgical treatment, but MRI of six patients was not available. The magnetic resonance (MR) sequences included unenhanced and gadolinium-enhanced T1-weighted imaging (T1WI), T2-weighted imaging (T2WI), and fluid-attenuated inversion recovery (FLAIR). The radiologic data included retrolabyrinthine regions involvement, focal bone destruction of the posterior aspect of the petrosal bone, tumor size, intratumoral residual bone, and expanded bone rim on CT, MRI signals, and extension and invasion of the adjacent structures.

All patients underwent surgical resection, and different surgical procedures were performed according to the different size, localization, and extension of the tumors. The procedures are outlined in Table 1. Three patients (cases 1, 13, 14) underwent subtotal resection because the tumors were firmly adherent to the critical structures and severe intraoperative bleeding was difficult to control. Post-operative radiotherapy was used with 70 Gy in 35 fractions in case 1 and 60 Gy in 30 fractions in case 14, but both of them still had recurrence later. Case 13 who did not receive radiotherapy underwent second surgery and also had recurrence. One patient (case 8) with VHL disease who had bilateral tumors underwent surgical resection with bilateral procedures and right cochlear implantation for hearing rehabilitation after resection. Pre-operative angiography was performed for five patients and pre-operative embolization of the tumors was performed in three cases.

Histopathologic analysis was performed for all the tumors. Routine paraffin-embedded tissue for HE and EnVision method was used for immunohistochemistry. Histopathologic finding was reviewed by a senior pathologist.

Results

Clinical findings

The clinical data are summarized in Table 1. Our series consisted of eight women and six men. Their ages ranged from 18 to 67 years (mean 42.3 years) at the time of diagnosis and 11–62 years (mean 35.2 years) at the time of initial symptoms. The mean interval between the time of first symptoms and diagnosis was 84.7 months (ranging from 10 to 216 months). Eleven patients presented with sporadic ELSTs. Three patients presented with VHL-associated ELSTs and they were all females and had a known family history of VHL disease. One of them had a retinal hemangioblastoma; another had multiple CNS hemangioblastomas; the last had a CNS hemangioblastoma and multiple renal cysts. Eight tumors were located in the left temporal bone and seven tumors in the right temporal bone (bilateral tumors were found in one patient with VHL disease). The most frequent cochleovestibular symptom was hearing loss in 14 patients (100%); other cochleovestibular symptoms were tinnitus in eight patients (57.1%), vertigo in three patients (21.4%), and aural fullness in three patients (21.4%). Ten patients (71.4%) presented with facial paralyses and five patients (14.3%) presented lower cranial nerve (glossopharyngeal, vagal, and hypoglossal nerve) deficits.

CT and MRI findings

Radiological findings of the tumors are summarized in Table 2. Tumor size was determined by measuring the largest diameter in any direction in CT images. The average diameter for all tumors (15 lesions in 14 patients) was 36.5 mm (ranging from 10.5 to 67.6 mm). CT findings revealed spiculated, stippled, or reticular high density within the tumors (Figs. 1a, 2, 3a, b, 4a and 5a). A thin high-density rim along the posterior margin of the tumor was identifiable in 6 of the 15 lesions, while it was subtler in other lesions (Figs. 1a, 2, 3a, b, 4a and 5a). Smaller lesions were centered in the endolymphatic sac and retrolabyrinthine regions of the posterior aspect of the petrosal bone (Fig. 2). Larger lesions extended into adjacent regions, such as mastoid cells, vertical facial nerve canal, semicircular canal, cochlea, tympanum, jugular foramen, internal auditory canal, and petrous apex (Figs. 1a, 3a, b, 4a and 5a). Available MRI showed eight lesions with solid or cystic-solid, heterogenous soft-tissue masses centered in the retrolabyrinthine region,

Table 1 Clinical data of 14 patients with endolymphatic sac tumor (ELST)

Case	VHL	Sex	Side	Age[a]	Cochleovestibular symptoms	Other symptoms	Surgical approach
1	N	M	L	26	Hearing loss and tinnitus 3 years	VII paralysis 5 months IX, X and XII deficit 2-month Cerebrospinal fluid otorrhea 5 days	Combined transtemporal-retrosigmoid approach
2	N	M	R	39	Hearing loss 10 years	VII deficits 5 months Earache and flowing blood 2 months	Infratemporal approach
3	N	M	L	45	Hearing loss, tinnitus and aural fullness 10 months	VII paralysis 5 months IX and X deficits 3 months	Translabyrinthine approach
4	N	F	L	64	Hearing loss and tinnitus 17 years Vertigo 10 years	VII paralysis 1 year IX and X deficits 2 months	Transcochlear approach with subtotal petrosectomy
5	N	F	R	34	Hearing loss and tinnitus 1 year	/	Translabyrinthine approach
6	N	M	L	67	Hearing loss and aural fullness 10 years	VII paralysis 9 months	Transcochlear approach with subtotal petrosectomy
7	N	M	R	58	Hearing loss and aural fullness 10 years	Flowing pus and blood 3 years IX and X deficits 2 months	Transcochlear approach
8	Y	F	L, R	29	L Hearing loss, tinnitus and vertigo 18 years; R Hearing loss and tinnitus 4 years	/	Transmastoid retrolabyrinthine approach
9	Y	F	L	18	Hearing loss 4 years	VII paralysis 1 year Earache and flowing pus 2 months	Combined transtemporal retrosigmoid approach
10	N	F	R	25	Hearing loss 10 years	VII paralysis 2 years Headache 1 year	Combined transtemporal retrosigmoid approach
11	N	F	L	63	Hearing loss 1 year	VII paralysis 6 months IX, X and XII deficits 1 month Headache 1 month	Combined Petroccipital transigmoid approach
12	N	F	R	43	Hearing loss, vertigo and tinnitus 6 years	/	Transmastoid retrolabyrinthine approach
13	N	F	R	59	Hearing loss and tinnitus 3 years	VII paralysis 1 month	Combined transmastoid and middle cranial fossa approach
14	N	F	L	22	Hearing loss and tinnitus 5 years	VII paralysis 2 years Flowing pus and blood 1 year	Combined transtemporal retrosigmoid approach

Y present, *N* absent, *M* male, *F* female, *L* left, *R* right, *VII* facial nerve, *IX* glossopharyngeal nerve, *X* pneumogastric nerve, *XII* hypoglossal nerve
[a]Age (years) at diagnosis

eight lesions with patchy and/or speckled hyperintensity on unenhanced T1WI (Figs. 1c, 4c and 5c), five lesions with flow voids on T2WI and T1WI (Fig. 4b), three lesions with blood fluid levels within cysts (Figs. 1b and 5b). On post-gadolinium T1WI, heterogeneous enhancement was revealed in all the lesions (Figs. 1d, 4d and 5d).

Surgical findings

Intra-operatively, the tumors were grayish-red or dark red, hypervascular and prone to bleeding when touched. Seven tumors were solid and eight tumors were cystic solid. The cysts were multilocular and sometimes filled with dark red or brown fluid in the capsules. The facial nerve canals were intact in four tumors; the facial nerve canals were destroyed but the lesions did not surround the facial nerves in two tumors; the facial nerves were partly surrounded but can be preserved after the lesions were separated in five tumors; the facial nerves were invaded and nerve graft or nerve anastomosis was performed in four tumors (the great auricular nerve graft in three cases, the facial nerve–hypoglossal nerve anastomosis in 1 case).

Histopathological findings

Light microscopy revealed most of the tumors with a papillary and glandular structure, which was lined by a single layer of flattened cuboidal-to-columnar cells with clear cytoplasm and without nuclear atypia (Figs. 1e and 4e). Some of the tumors showed cystic cavities filled with colloid-like material. Immunohistochemically, cytokeratin was positive in 15 lesions (100%), vimentin positive in 10 (66.7%), S-100 positive in 7 (46.7%), and thyroglobulin and transcription termination factor 1 negative in all lesions. The proliferation rate as assessed by the Ki67 immunostain was < 1.0–25.0%.

Table 2 Radiological features of 14 patients with ELST

Case	Size (mm)	CT characteristics			MRI characteristics			
		Intratumoral residual bone	Posterior expanded bone rim	Bone destruction	T2WI	T1WI hyperintense	Flow voids	Enhancement
1	67.6	Spiculated	Subtle	PSPB, PSC, ASC, HSC, cochlea, FNC, IAC, mastoid cells, tympanum, petrous apex, jugular foramen, HC	NA	NA	NA	NA
2	34.7	Spiculated	Subtle	PSPB, FNC, IAC, mastoid cells, tympanum, jugular foramen, HC	Mixed BFL	Present	Absent	Heterogeneous
3	19.2	Stippled	Identifiable	PSPB, FNC, IAC, jugular foramen, mastoid cells	Mixed	Present	Absent	Heterogeneous
4	42.4	Spiculated, reticular	Identifiable	PSPB, FNC, IAC, mastoid cells, tympanum, jugular foramen	Mixed BFL	Present	Present	Heterogeneous
5	23.6	Reticular	Identifiable	PSPB, jugular foramen, mastoid cells	Mixed	Present	Absent	Heterogeneous
6	41.5	Spiculated, reticular	Subtle	PSPB, FNC, IAC, mastoid cells, tympanum, jugular foramen	Mixed	Present	Present	Heterogeneous
7	39.6	Spiculated, reticular	Subtle	PSPB, PSC, FNC, IAC, mastoid cells, tympanum, petrous apex, jugular foramen	Mixed	Present	Present	Heterogeneous
8	L20.1	Reticular	Subtle	PSPB, mastoid cells	NA	NA	NA	NA
	R19.3	Reticular	Identifiable	PSPB, mastoid cells	NA	NA	NA	NA
9	47.5	Spiculated	Subtle	PSPB, PSC, ASC, HSC, cochlea, FNC, IAC, mastoid cells, tympanum, petrous apex, jugular foramen	NA	NA	NA	NA
10	38.7	Spiculated	Identifiable	PSPB, PSC, ASC, HSC, cochlea, FNC, IAC, mastoid cells, tympanum, petrous apex, jugular foramen	NA	NA	NA	NA
11	50.5	Stippled, reticular, spiculated	Subtle	PSPB, PSC, FNC, IAC, mastoid cells, tympanum, petrous apex, jugular foramen, HC	Mixed BFL	Present	Present	Heterogeneous
12	10.5	Stippled	Identifiable	PSPB	Mixed	Present	Absent	Heterogeneous
13	41.2	Spiculated	Subtle	PSPB, PSC, ASC, HSC, cochlea, FNC, IAC, mastoid cells, tympanum, petrous apex, jugular foramen, HC	Mixed	Present	Present	Heterogeneous
14	51.5	Spiculated Reticular	subtle	PSPB, PSC, ASC, HSC, cochlea, FNC, IAC, mastoid cells, tympanum, petrous apex, jugular foramen	NA	NA	NA	NA

PSPB posterior surface of petrous bone, *FNC* facial nerve canal, *IAC* internal auditory canal, *PSC* posterior semicircular canal, *ASC* anterior semicircular canal, *HSC* horizontal semicircular canal, *HC* hypoglossal canal, *BFL* blood fluid level, *NA* not available

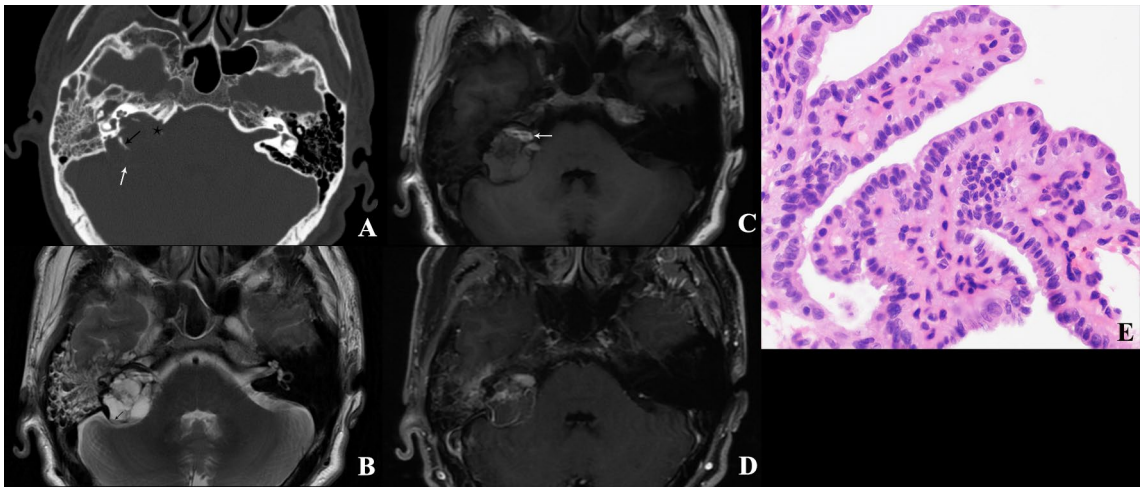

Fig. 1 Patient 2. **a** Axial CT scan through internal auditory canal shows irregular bone destruction in the posterior labyrinth of the right petrous bone, with spiculated residual bone in the tumor (black arrow). The expanded bony rim along the posterior margin of the tumor is subtle (white arrow). The tumor involves the internal auditory canal (black asterisk). **b** Axial T2WI shows the predominantly multicystic appearance of the tumor and the blood fluid level within one of the cysts (black arrow). **c** Unenhanced axial T1WI shows a few scattered areas of hyperintensity in the tumor (white arrow). **d** Enhanced axial T1WI shows heterogeneous enhancement of the tumor. **e** Microphotograph of the tumor shows the papillary-type area lined by cubic or columnar epithelial cells. The tumor cells are monolayer and the nuclei are at the same level (HE × 400)

Fig. 2 Patient 8. Axial CT scan through cochlear aqueduct shows bilateral tumors in one patient with VHL disease. Both lesions are centered in the retrolabyrinthine regions of the posterior aspect of the petrosal bone. The intratumoral bone remnants of the destroyed petrous bone are reticular in both lesions. The expanded bony rim along the posterior margin is subtle in the left lesion (white arrow), but it is identifiable in the right lesion (black arrow)

Discussion

Anatomy and function of endolymphatic sac

ELSTs are aggressive papillary adenomatous tumors originating from the endolymphatic sac [1]. The endolymphatic duct runs in the osseous vestibular aqueduct and becomes expanded to form the endolymphatic sac situated under the dura of the petrous bone. The endolymphatic sac is a component of the membranous labyrinth and plays important roles in regulating inner ear endolymph and maintaining vestibular function [11]. Endolymph is resorbed into the cerebrospinal fluid from the endolymphatic sac. Obstruction or damage to the endolymphatic sac may cause endolymph to accumulate and produce hydrops, which result in vestibular and cochlear dysfunction, such as Meniere's disease [12].

The endolymphatic sac has two parts: (a) a rugose or intermediate segment, and (b) a distal sac. The rugose segment is contiguous with the endolymphatic duct and partially covered by bone [11]; ELSTs usually arise from this part [13, 14]. The distal part of the endolymphatic sac is ensheathed by two layers of the dura in the posterior cranial fossa.

Clinical features

ELSTs occur mostly in adults and usually present in the third and fourth decades of life, over a wide age range from 4 to 85 years [3, 13, 15–17]. About 3% to 15% of cases are associated with VHL [18, 19]. Bilateral tumors are seen in nearly one-third patients who have VHL-associated ELSTs [20]. One article reported that the mean age of the patients with sporadic ELSTs was 52.5 years, whereas it was 31.3 years in the patients with associated VHL [21]. There may be a

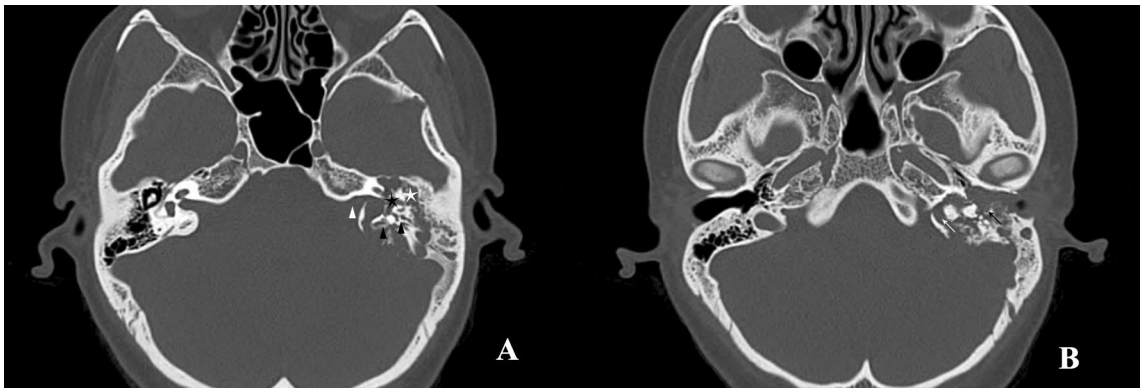

Fig. 3 Patient 9. Axial CT scans through internal auditory canal (**a**) and jugular foramen (**b**) show moth-eaten bone erosion in the left petrous bone, with spiculated residual bone in the tumor. The expanded bony rim along the posterior margin of the tumor is subtle. The tumor involves the internal auditory canal (white arrowhead), semicircular canal (black arrowhead), cochlea (black asterisk), tympanum (white asterisk), jugular foramen (white arrow), and facial nerve canal (black arrow)

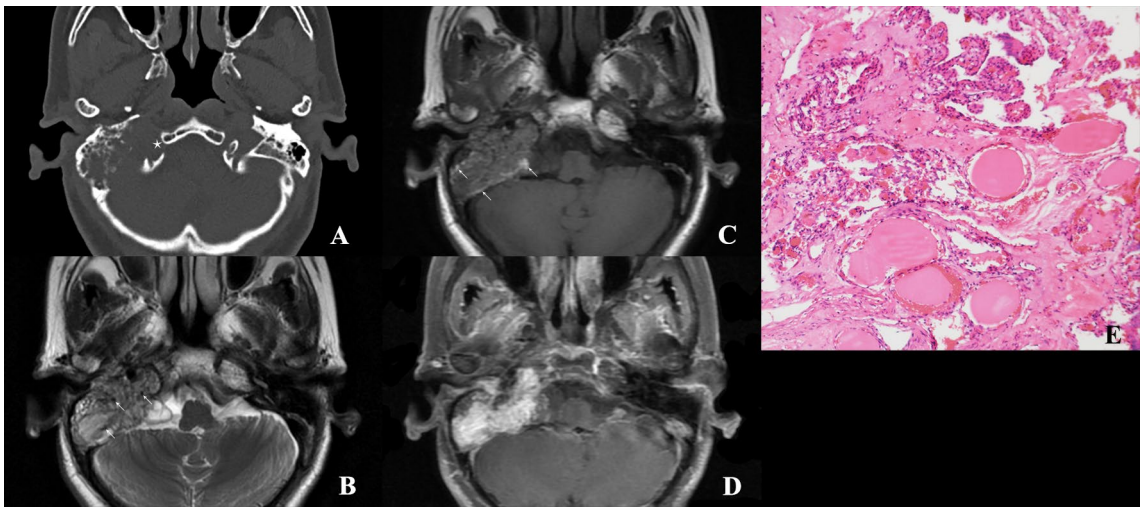

Fig. 4 Patient 11. **a** Axial CT scan through hypoglossal canal shows irregular bone destruction in the right petrous bone, with stippled, reticular and spiculated residual bone in the tumor. The tumor involves the hypoglossal canal (white asterisk). **b** Axial T2WI shows the predominantly solid appearance of the tumor with flow voids (white arrow). **c** Unenhanced axial T1WI shows a few scattered areas of hyperintensity in the tumor (white arrow). **d** Enhanced axial T1WI shows heterogeneous and avid enhancement of the tumor. **e** Microphotograph of the tumor shows the papillary cystic glandular structure of endolymphatic sac tumor. The fibrous stroma of the papillary fronds is rich in vasculatures (HE × 100)

slight female predominance [1]. In the present study, the average age at the time of diagnosis was 42.2 years with the female-to-male ratio being 1.33:1, which is consistent with the findings of the previous studies [3, 6, 13, 16, 17]; the three patients with associated VHL were all females, one of which had bilateral ELSTs.

Because of the slow-growing nature of the tumor, the interval between the first symptoms and the diagnosis is long. The most common initial symptom is cochleovestibular dysfunction. Hearing loss that presents in nearly all patients may be sudden or gradual [22, 23]. Other common symptoms include tinnitus, vertigo, and aural fullness. The cochleovestibular symptoms mimic Meniere's disease, which may delay the diagnosis [3, 23]. There were three cases (21.4%) initially misdiagnosed as Meniere's disease in the present study. Among the cranial nerves, the facial nerve is involved most often, followed by the glossopharyngeal, vagal, and trigeminal nerves [23–25]. In this study, the most common cranial nerve deficit was facial palsy, followed by lower cranial nerves. We had no case of trigeminal nerve deficit.

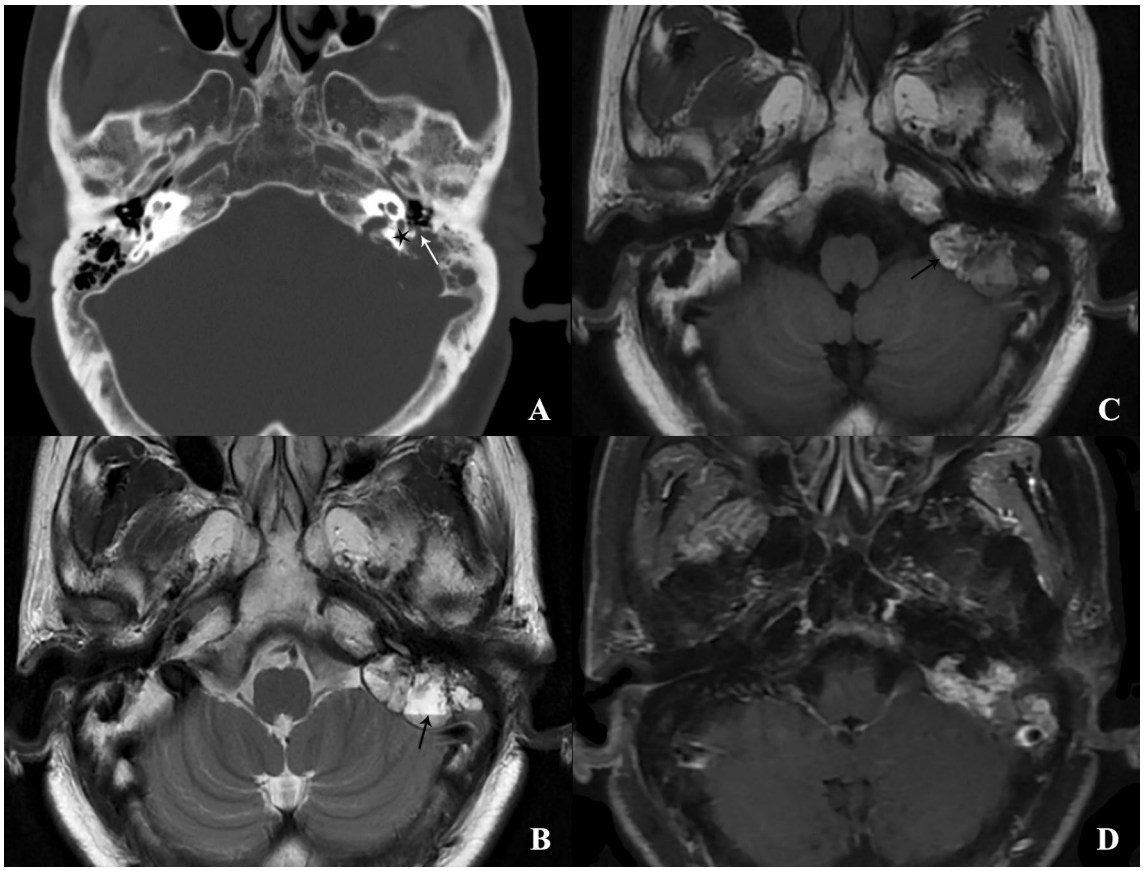

Fig. 5 Patient 4. **a** Axial CT scan through fenestra vestibuli shows irregular bone destruction in the left petrous bone, with reticular and spiculated residual bone in the tumor. The tumor involves the semicircular canal (black asterisk) and facial nerve canal (white arrow). **b** Axial T2WI shows a blood fluid level in the tumor (black arrow). **c** Unenhanced axial T1WI shows patchy hyperintensity in the tumor (black arrow). **d** Enhanced axial T1WI shows heterogeneous enhancement of the tumor

Radiological manifestation

Radiology is important for diagnosis and pre-operative evaluation of ELSTs. HRCT can clearly show bone destructions caused by tumors, especially destructions of facial nerve canal, jugular foramen, hypoglossal canal, and internal auditory canal. MRI has excellent sensitivity and resolution for soft tissue, so it can accurately exhibit the extent of the tumor.

On CT, geographic or moth-eaten bone destruction can be seen in the posterior labyrinth of the petrous bone, with stippled, spiculated or reticular high density in the tumor [17, 26]. The intratumoral high density stipples, spicules, and reticulations represent residual bone fragments caused by tumor infiltration rather than new ossification or calcification, because ELSTs do not produce osteoid, cartilaginous matrix, or ectopic calcium deposits at histopathologic examination [5, 6]. Our series also showed stippled, spiculated or reticular intratumoral residual bone in all tumors. There is a thin high-density rim along the posterior margin of the lesion, which may represent the expanded cortex of the petrous bone [17, 27]. This expanded appearance may represent its low-grade malignant and slow-growing nature. In the present study, the thin high-density rim was subtler in 9 of the 15 lesions. The possible reason is the noise effect of HRCT scan or the thin rim being destructed.

MRI can excellently show the prominent characteristics of hypervascularity and intratumoral hemorrhage of ELSTs: (1) hyperintense rim or foci regions on non-contrast T1WI but hyperintense, isointense or hypointense on T2WI; (2) moderate to strong heterogeneous enhancement on post-contrast T1WI in the solid regions; (3) blood fluid levels in the capsules of some cystic components; and (4) flow voids on T1WI and T2WI in some large tumors [17, 22, 23, 28–30]. In our series, intra-operative findings of the grayish-red or dark red hypervascular appearance, easy bleeding when touched and dark red or brown fluid in some capsules also suggested these characteristics. On the available MRI of eight cases, ELSTs presented hyperintense focal signals on non-contrast T1WI in all cases, blood fluid levels on T2WI in three cases, and flow voids on T1WI and T2WI in three cases.

Clinicoradiological correlation

ELSTs arise from the endolymphatic sac, so they exhibit an epicenter in the retrolabyrinthine area. CT and MRI show a tissue mass centered in the retrolabyrinthine region, eroding the posterior surface of petrous bone. The tumor within the endolymphatic sac can block normal endolymphatic fluid resorption and disrupt its homeostasis, resulting in intralabyrinthine hemorrhage followed by inflammation and endolymphatic hydrops, and then cause the development of cochleovestibular symptoms, including hearing loss, tinnitus, and vertigo [3, 22, 31]. As the ELST grows, it can aggravate the endolymphatic hydrops or invade labyrinth system directly, which leads to a more gradual progression of cochleovestibular dysfunction. At that stage, the destructions of semicircular canal, cochlea or even ossicles in tympanum can be exhibited on CT.

There are four potential vectors for tumor extension: medial, lateral, superior, and anteromedial [23, 29]. Tumors often grow laterally toward the middle ear via transmastoid route. CT can show bone erosions of mastoid, vertical segment of facial nerve canal, posterior semicircular canal, and tympanum. Patients may have facial palsy or produce symptoms that mimic chronic otitis media. In our series, two cases were misdiagnosed with chronic otitis media before imaging examination; 11 patients involved facial nerve canal on CT, 10 of them (90.9%) had facial paralysis. The total incidence rate (71.4%) of facial paralyses was higher than previous studies [22, 29]. The possible explanation was that most of the patients in our series did not undergo radiological scanning when they presented with cochleovestibular symptoms until facial paralyses.

Medial extension to the cerebellopontine angle region or posterior fossa is another common growth pathway. CT and MRI may show destructions of jugular foramen, internal auditory canal, and lateral part of occipital bone. We observed different degrees of bone destructions of jugular foramen in 12 cases, but only five patients (41.7%) had glossopharyngeal and vagal nerve deficits; destructions of hypoglossal canal were observed in four cases and two patients (50%) had hypoglossal nerve deficits. MRI may also exhibit brainstem and cerebellum compression and distortion. If the tumors are large enough, brainstem compression may contribute to poor vestibular function and cause headache [22]. MRI showed brainstem compression in one case and the patient had headache in our series.

A few tumors can extend superiorly through the semicircular canals and into the middle cranial fossa, which may contribute to headache secondary to brain compression [3]. In our series, CT demonstrated a tumor invading the middle cranial fossa in one case and the patient had related symptom.

Finally, anteromedial extension along the petrous ridge may invade the basilar clivus, cavernous sinus, or sphenoid sinus and contribute to trigeminal nerve deficit [32]. There was no such case in our series.

It is worth mentioning that multiple growth patterns can be observed in large tumors. The typical pattern was the combination of lateral and medial growth directions destroying the middle ear and invading the cerebellopontine angle region. Patients may have facial nerve, glossopharyngeal verve, vagal nerve or hypoglossal nerve deficits besides cochleovestibular symptoms. The mean time between the first symptoms and the diagnosis was 84.7 months, which indicated that many of the patients presented late with advanced stage disease. Thus, to identify ELSTs early and ensure greater potential for hearing preservation, imaging tests should be performed as early as possible in patients with cochleovestibular symptoms, particularly when other diseases such as Meniere's disease, otitis media, and central nervous system disease cannot explain the symptoms.

Treatment modalities

The primary modality of treatment for ELSTs is extensive surgery with negative margins. The size of the tumors and aforementioned pathways of tumor invasion should be considered when planning the surgical approach. Small tumors localized to the endolymphatic sac area with no extension in the surrounding subsites can be dealt with by the transmastoid retrolabyrinthine approach; large tumors with labyrinthine invasion require the translabyrinthine approach with facial nerve preservation; larger tumors involving the facial nerve, the jugular bulb, and the middle ear need infratemporal approach; tumors with deeper involvement of the petrous bone need transcochlear approach; tumors involving the posterior and middle cranial fossa require combined transtemporal retrosigmoid approach or even subtotal resection of the temporal bone for adequate exposure [30, 28, 29, 33].

Abdominal fat is used to fill the surgical residual cavity and dural substitute is used to seal the dura to prevent cerebrospinal fluid leaks if the dura is partially excised. The great auricular nerve is used for nerve graft, or a facial nerve–hypoglossal nerve anastomosis is performed if the tumors involve the facial nerves. Post-operative radiotherapy seems to have a limited role in long-term prognosis for patients, but may give some beneficial results in subtotal resection (a roughly 50% risk of tumor regrowth) [28, 34]. In cases of bilateral ELSTs who have VHL disease, cochlear implantation may be a viable option for hearing rehabilitation, but the tumor has to be resected before it reaches and destroys the cochlea and the posterior labyrinth [28, 30].

On the basis of the prominent feature of hypervascularity, pre-operative embolization may be helpful to prevent intra-operative bleeding, minimize morbidities, and facilitate

complete resection. The blood supply arises predominantly from the branches of the external carotid artery, such as posterior auricular artery, occipital artery, and ascending pharyngeal artery, but may also arise from the branches of the vertebral artery and the internal carotid artery in larger tumors [3, 23, 29, 32].

Differential diagnosis

ELSTs must be differentiated from other tumors in petrous bone and cerebellopontine angle, which have similar clinical and radiological appearance as ELSTs. This group includes: paragangliomas, meningiomas, acoustic neuromas, middle ear carcinomas and choroid plexus papillomas.

The primary locations of the lesions will be helpful for the differential diagnosis. The center or the epicenter of ELSTs is in the retrolabyrinthine region. Temporal bone paragangliomas are normally located in the region of the jugular foramen and on the promontory along the Jacobson nerve [35]. Meningiomas and acoustic neuromas are typically located at the cerebellopontine angle [36, 37]. Middle ear carcinomas are mainly located in the tympanum, tympanic sinus, and deep within the external auditory canal [38]. Choroid plexus papillomas that arise from the lateral foramen of Luschka may involve the cerebellopontine angle, but they are intradural tumors that do not exhibit osseous invasion, and thus lack the osseous erosion that is characteristic of ELSTs [23]. If the lesions are too large and extend to multiple directions, the initial locations are difficult to discriminate. However, ELSTs have characteristic imaging features (intratumoral bone spicules and posterior expanded bone rim on CT; hyperintense foci on non-contrast T1WI), which are unusual in other tumors [3, 17, 23, 27, 28, 37–39].

Conclusion

Pre-operative diagnosis and evaluation of ELSTs mainly depend on radiology. Imaging tests should be performed to identify ELSTs early and ensure greater potential for hearing preservation particularly in patients with cochleovestibular symptoms followed by facial nerve and lower cranial nerve deficits. If radiology shows bone destructions centered in retrolabyrinthine with intratumoral residual bone spicules on CT and the prominent features of hypervascularity and intratumoral hemorrhage on MRI, ELSTs should be diagnosed.

Compliance with ethical standards

Conflict of interest We declare that we have no financial and personal relationships with other people or organizations that can inappropriately influence our work, there is no professional or other personal interest of any nature or kind in any product, service and/or company that could be construed as influencing the position presented in, or the review of, the manuscript entitled "Clinicoradiologic Characteristics of Endolymphatic Sac Tumors".

References

1. EI-Naggar AK, Chan JKC, Grandis JR, Takata T, Slootweg PJ et al (2017) WHO classification of tumours of the head and neck. Tumours of the ear, 4th edn. IARC Press, Lyon
2. Du J, Wang J, Cui Y, Zhang C, Li G, Fang J, Yue S, Xu L (2015) Clinicopathologic study of endolymphatic sac tumor (ELST) and differential diagnosis of papillary tumors located at the cerebellopontine angle. Neuropathology 35(5):410–420. https://doi.org/10.1111/neup.12200
3. Megerian CA, Semaan MT (2007) Evaluation and management of endolymphatic sac and duct tumors. Otolaryngol Clin N Am 40(3):463–478. https://doi.org/10.1016/j.otc.2007.03.002
4. Hassard AD, Boudreau SF, Cron CC (1984) Adenoma of the endolymphatic sac. J Otolaryngol 13(4):213–216
5. Gaffey MJ, Mills SE, Fechner RE, Intemann SR, Wick MR (1988) Aggressive papillary middle-ear tumor. A clinicopathologic entity distinct from middle-ear adenoma. Am J Surg Pathol 12(10):790–797. https://doi.org/10.1097/00000478-198810000-00009
6. Heffner DK (1989) Low-grade adenocarcinoma of probable endolymphatic sac origin A clinicopathologic study of 20 cases. Cancer 64(11):2292–2302. https://doi.org/10.1002/1097-0142(19891201)64:11%3c2292:AID-CNCR6%3e3.0.CO;2-%23
7. Li JC, Brackmann DE, Lo WWM, Carberry JN, House JW (1993) Reclassification of aggressive adenomatous mastoid neoplasms as endolymphatic sac tumors. Laryngoscope 103(12):1342–1348. https://doi.org/10.1288/00005537-199312000-00004
8. Lonser RR, Glenn GM, Walther MM, Chew EY, Libutti SK, Linehan WM, Oldfield EH (2003) von Hippel–Lindau disease. Lancet 361(9374):2059–2067. https://doi.org/10.1016/S0140-6736(03)13643-4
9. Poulsen MLM, Gimsing S, Kosteljanetz M, Moller HU, Brandt CA, Thomsen C, Bisgaard ML (2011) von Hippel–Lindau disease: surveillance strategy for endolymphatic sac tumors. Genet Med 13(12):1032–1041. https://doi.org/10.1097/GIM.0b013e31822beab1
10. Ganeshan D, Menias CO, Pickhardt PJ, Sandrasegaran K, Lubner MG, Ramalingam P, Bhalla S (2018) Tumors in von Hippel–Lindau syndrome: from head to toe-comprehensive state-of-the-art review. RadioGraphics 38(3):849–866. https://doi.org/10.1148/rg.2018170156
11. Ammirati M, Spallone A, Feghali J, Ma J, Cheatham M, Becker D (1995) The endolymphatic sac: microsurgical topographic anatomy. Neurosurgery 36(2):416–419. https://doi.org/10.1097/00006123-199502000-00028
12. Sajjadi H, Paparella M (2008) Meniere's disease. Lancet 372(9636):406–414. https://doi.org/10.1016/S0140-6736(08)61161-7
13. Ferreira MAT, Feiz-Erfan I, Zabramski JM, Spetzler RF, Coons SW, Preul MC (2002) Endolymphatic sac tumor: unique features of two cases and review of the literature. Acta Neurochir 144(10):1047–1053. https://doi.org/10.1007/s00701-002-0969-7
14. Kempermann G, Neumann HPH, Volk B (1998) Endolymphatic sac tumours. Histopathology 33(1):2–10. https://doi.org/10.1046/j.1365-2559.1998.00460.x
15. Kupferman ME, Bigelow DC, Carpentieri DF, Bilaniuk LT, Kazahaya K (2004) Endolymphatic sac tumor in a 4-year-old boy. Otol Neurotol 25(5):782–786. https://doi.org/10.1097/00129492-200409000-00022

16. Devaney KO, Boschman CR, Willard SC, Ferlito A, Rinaldo A (2005) Tumours of the external ear and temporal bone. Lancet Oncol 6(6):411–420. https://doi.org/10.1016/S1470-2045(05)70208-4
17. Mukherji SK, Albernaz VS, Lo WWM, Gaffey MJ, Megerian CA, Feghali JG, Brook AL, Lewin JS, Lanzieri CF, Talbot JM (1997) Papillary endolymphatic sac tumors: CT, MR imaging, and angiographic findings in 20 patients. Radiology 202(3):801–808. https://doi.org/10.1148/radiology.202.3.9051037
18. Bausch B, Wellner U, Peyre M, Boedeker CC, Hes FJ, Anglani M, de Campos JM, Kanno H, Maher ER, Krauss T (2016) Characterization of endolymphatic sac tumors and von Hippel–Lindau disease in the international ELST registry. Head Neck 38(S1):E673–E679. https://doi.org/10.1002/hed.24067
19. Dornbos D, Kim HJ, Butman JA, Lonser RR (2018) Review of the neurological implications of von Hippel–Lindau disease. JAMA Neurol 75(5):620–627. https://doi.org/10.1001/jamaneurol.2017.4469
20. Manski TJ, Heffner DK, Glenn GM et al (1997) Endolymphatic sac tumors: a source of morbid hearing loss in von Hippel–Lindau disease. JAMA 277(18):1461–1466. https://doi.org/10.1001/jama.1997.03540420057030
21. Bambakidis NC, Megerian CA, Ratcheson RA (2004) Differential grading of endolymphatic sac tumor extension by virtue of von Hippel–Lindau disease status. Otol Neurotol 25(5):773–781. https://doi.org/10.1097/00129492-200409000-00021
22. Wick CC, Manzoor NF, Semaan MT, Megerian CA (2015) Endolymphatic sac tumors. Otolaryngol Clin N Am 48(2):317–330. https://doi.org/10.1016/j.otc.2014.12.006
23. Bell D, Gidley P, Levine N, Fuller GN (2011) Endolymphatic sac tumor (aggressive papillary tumor of middle ear and temporal bone): sine qua non radiology-pathology and the University of Texas MD Anderson Cancer Center experience. Ann Diagn Pathol 15(2):117–123. https://doi.org/10.1016/j.anndiagpath.2010.08.009
24. Friedman RA, Hoa M, Brackmann DE (2013) Surgical management of endolymphatic sac tumors. J Neurol Surg Part B Skull Base 74(1):12–19. https://doi.org/10.1055/s-0032-1329622
25. Butman JA, Kim HJ, Baggenstos M, Ammerman JM, Dambrosia J, Patsalides A, Patronas NJ, Oldfield EH, Lonser RR (2007) Mechanisms of morbid hearing loss associated with tumors of the endolymphatic sac in von Hippel–Lindau disease. JAMA 298(1):41–48. https://doi.org/10.1001/jama.298.1.41
26. Lo WW, Applegate LJ, Carberry JN, Soltibohman LG, House JW, Brackmann DE, Waluch V, Li JC (1993) Endolymphatic sac tumors: radiologic appearance. Radiology 189(1):199–204. https://doi.org/10.1148/radiology.189.1.8372194
27. Patel NP, Wiggins RH 3rd, Shelton C (2006) The radiologic diagnosis of endolymphatic sac tumors. Laryngoscope 116(1):40–46. https://doi.org/10.1097/01.mlg.0000185600.18456.36
28. Poletti AM, Dubey SP, Barbo R, Pericotti S, Fiamengo B, Colombo G, Scorsetti M, Lorusso R, Mazzoni A (2013) Sporadic endolymphatic sac tumor: its clinical, radiological, and histological features, management, and follow-up. Head Neck 35(7):1043–1047. https://doi.org/10.1002/hed.22962
29. Mendenhall WM, Suárez C, Skálová A, Strojan P, Triantafyllou A, Devaney KO, Williams MD, Rinaldo A, Ferlito A (2018) Current treatment of endolymphatic sac tumor of the temporal bone. Adv Ther 35(7):887–898. https://doi.org/10.1007/s12325-018-0730-0
30. Zanoletti E, Girasoli L, Borsetto D, Opocher G, Mazzoni A, Martini A (2017) Endolymphatic sac tumour in von Hippel–Lindau disease: management strategies. Acta Otorhinolaryngol Ital 37(5):423–429. https://doi.org/10.14639/0392-100x-1402
31. Jagannathan J, Butman JA, Lonser RR, Vortmeyer AO, Zalewski CK, Brewer C, Oldfield EH, Kim HJ (2007) Endolymphatic sac tumor demonstrated by intralabyrinthine hemorrhage. J Neurosurg 107(2):421–425. https://doi.org/10.3171/jns-07/08/0421
32. Janse van Rensburg P, van der Meer G (2008) Magnetic resonance and computed tomography imaging of a grade IV papillary endolymphatic sac tumour. J Neurooncol 89(2):199–203. https://doi.org/10.1007/s11060-008-9605-6
33. Schipper J, Maier W, Rosahl SK, van Velthoven V, Berlis A, Boedeker CC, Laszig R, Teszler CB, Ridder GJ (2006) Endolymphatic sac tumours: surgical management. J Otolaryngol 35(6):387–394. https://doi.org/10.2310/7070.2006.0082
34. Diaz RC (2011) Head and neck: ear: endolymphatic Sac Tumor (ELST). Atlas Genet Cytogenet Oncol Haematol 14(3):321–326. https://doi.org/10.4267/2042/44722
35. Suárez C, Sevilla MA, Llorente JL (2007) Temporal paragangliomas. Eur Arch Otorhinolaryngol 264(7):719–731. https://doi.org/10.1007/s00405-007-0267-3
36. Semaan MT, Wick CC, Kinder KJ, Stuyt JG, Chota RL, Megerian CA (2016) Retrosigmoid versus translabyrinthine approach to acoustic neuroma resection: a comparative cost-effectiveness analysis. Laryngoscope 126(S3):S5–S12. https://doi.org/10.1002/lary.25729
37. Coffey N, Torres C, Glikstein R, Al Mansoori T, del Carpio-O'Donovan R, Patro S (2017) Imaging findings in sensorineural hearing loss: a pictorial essay. Can Assoc Radiol J 68(2):106–115. https://doi.org/10.1016/j.carj.2015.12.001
38. Zhang F, Sha Y (2013) Computed tomography and magnetic resonance imaging findings for primary middle-ear carcinoma. J Laryngol Otol 127(6):578–583. https://doi.org/10.1017/S0022215113000923
39. Nevoux J, Nowak C, Vellin J, Lepajolec C, Sterkers O, Richard S, Bobin S (2014) Management of endolymphatic sac tumors: sporadic cases and von Hippel–Lindau disease. Otol Neurotol 35(5):899–904. https://doi.org/10.1097/MAO.0000000000000299